Reconfigurable Intelligent Surface Aided Wireless Sensing for Scene Depth Estimation



Abdelrahman Taha
a.taha@asu.edu

Hao Luo
h.luo@asu.edu

Ahmed Alkhateeb
alkhateeb@asu.edu

Wireless Intelligence Lab, Arizona State University

IEEE International Conference on Communications (ICC), 2023

IRA A. FULTON SCHOOLS OF engineering
ARIZONA STATE UNIVERSITY

Wireless Intelligence Lab

Challenges with scene depth estimation

Depth estimation

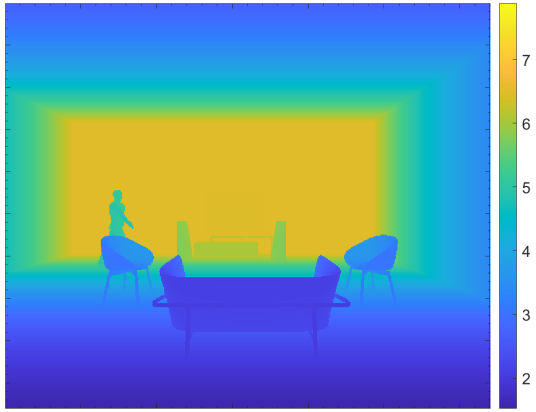

- Measure the distance between
  - The surface of the object
  - The sensor
- Enable some emerging applications
  - Augmented and virtual reality
  - Autonomous vehicles

Optical sensing

- Good depth accuracy
- Depth accuracy degrades
  - Unfavorable light conditions
  - Shiny, dark, or transparent targets
  - Around-the-corner targets
- Key privacy concerns
- Depth estimation ambiguity for distant targets

These motivates research for other technologies to accurately sense the environment

Wireless sensing for scene depth estimation

Wireless sensing

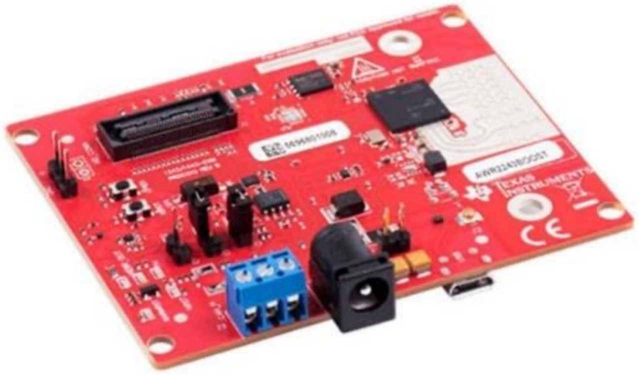

- Different propagation properties (mmWave)
  - Unaffected by light sources
  - Shiny, dark, or transparent targets
  - Around-the-corner targets
- Fewer privacy concerns
- Detect more distant targets
- mmWave MIMO based wireless sensing [Taha'21]

Optical sensing

- Good depth accuracy
- Depth accuracy degrades
  - Unfavorable light conditions
  - Shiny, dark, or transparent targets
  - Around-the-corner targets
- Key privacy concerns
- Depth estimation ambiguity for distant targets

Scaling mmWave MIMO antenna array requires large hardware complexity

[T
Reality," in *IEEE Access*, vol. 9, pp. 48341-48363, 2021.

Reconfigurable intelligent surface aided wireless sensing

Wireless sensing

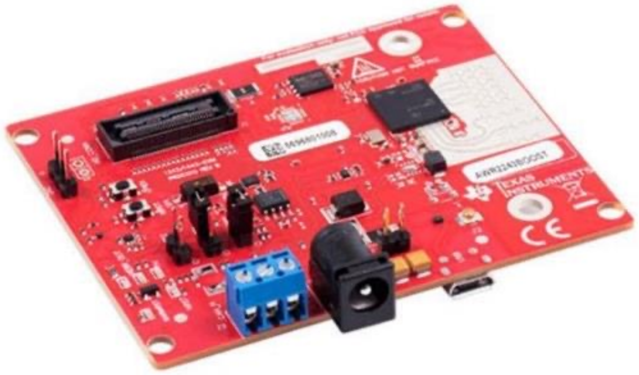

- Different propagation properties (mmWave)
  - Unaffected by light sources
  - Shiny, dark, or transparent targets
  - Around-the-corner targets
- Fewer privacy concerns
- Detect more distant targets

Reconfigurable intelligent surface

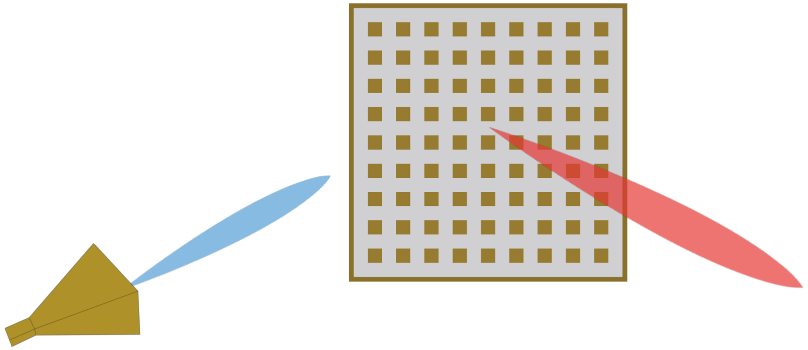

- Control propagation of radio waves → extend coverage
- Nearly-passive elements → energy-efficient architecture
- Massive number of elements → fine-grained beams

RIS can provide a high spatial resolution for scene depth estimation!

System model

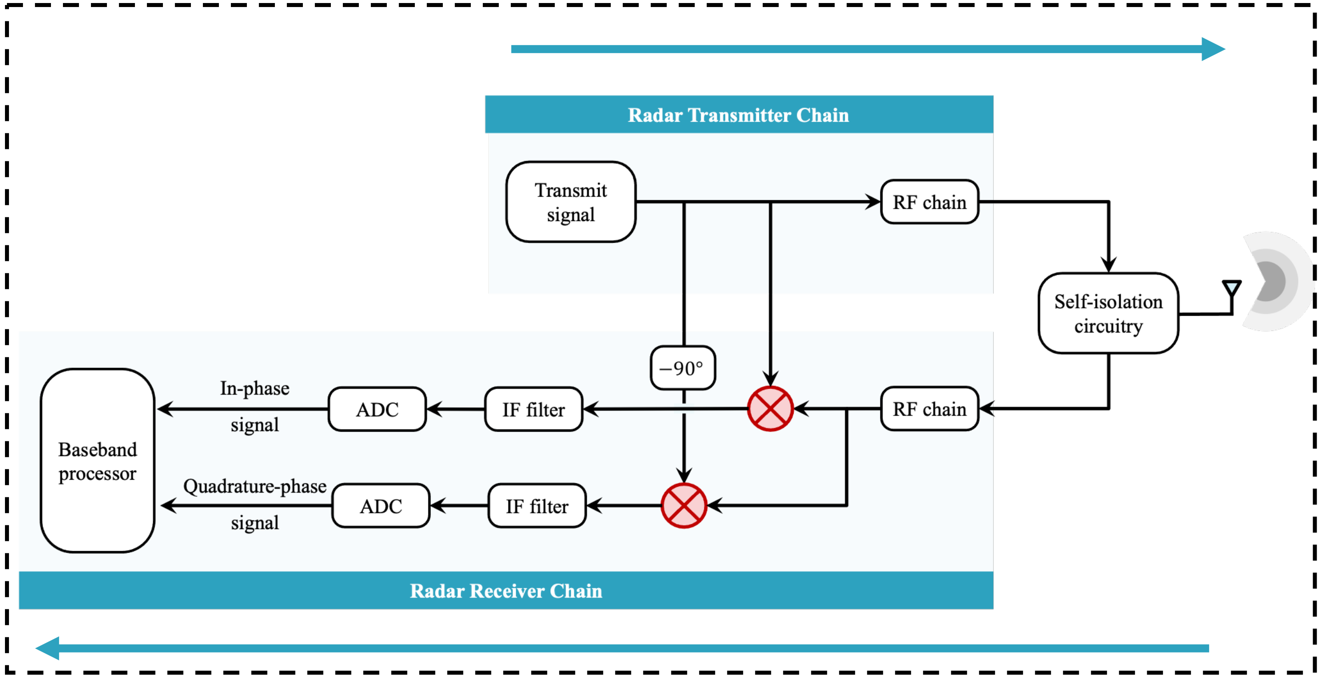

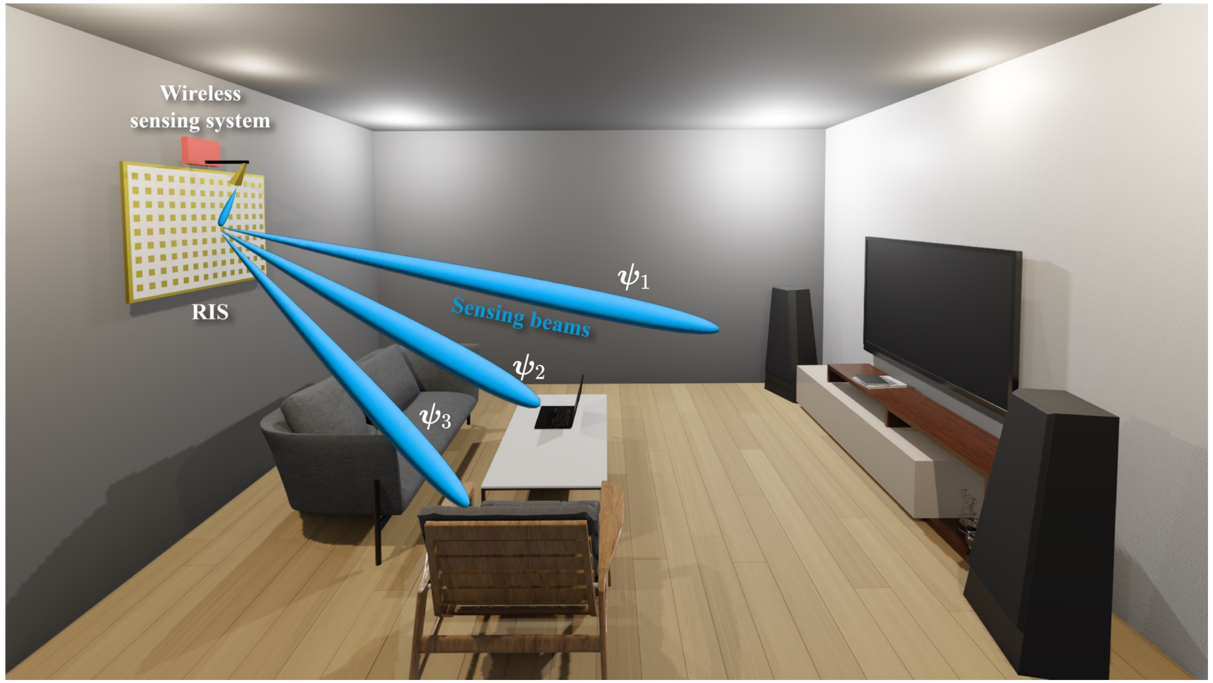

Adopted wireless sensing system

- Wideband FMCW radar transceiver with a complex-baseband architecture
- Tx and Rx: connected through a self-isolation circuitry to a shared single antenna
- Transmit signal: radar frame of M_{chirp} repeated chirp signals
- Channel model: wideband geometric channel model

System model (cont.)

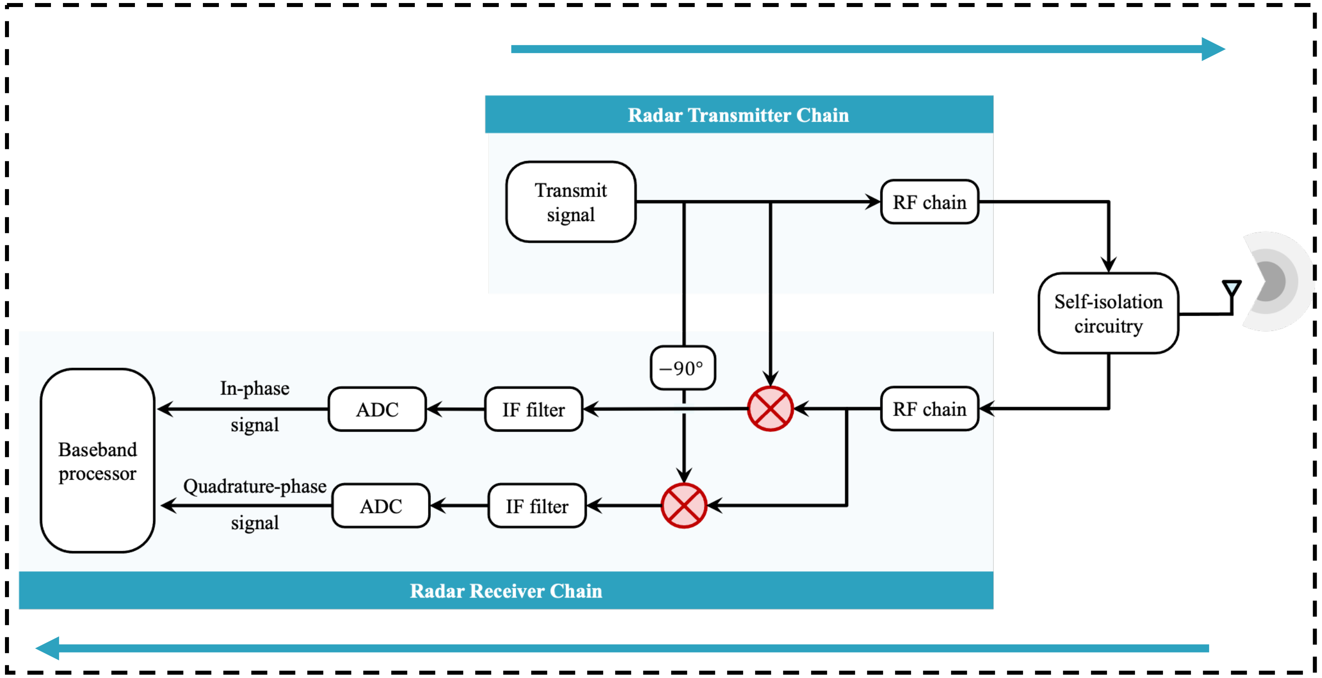

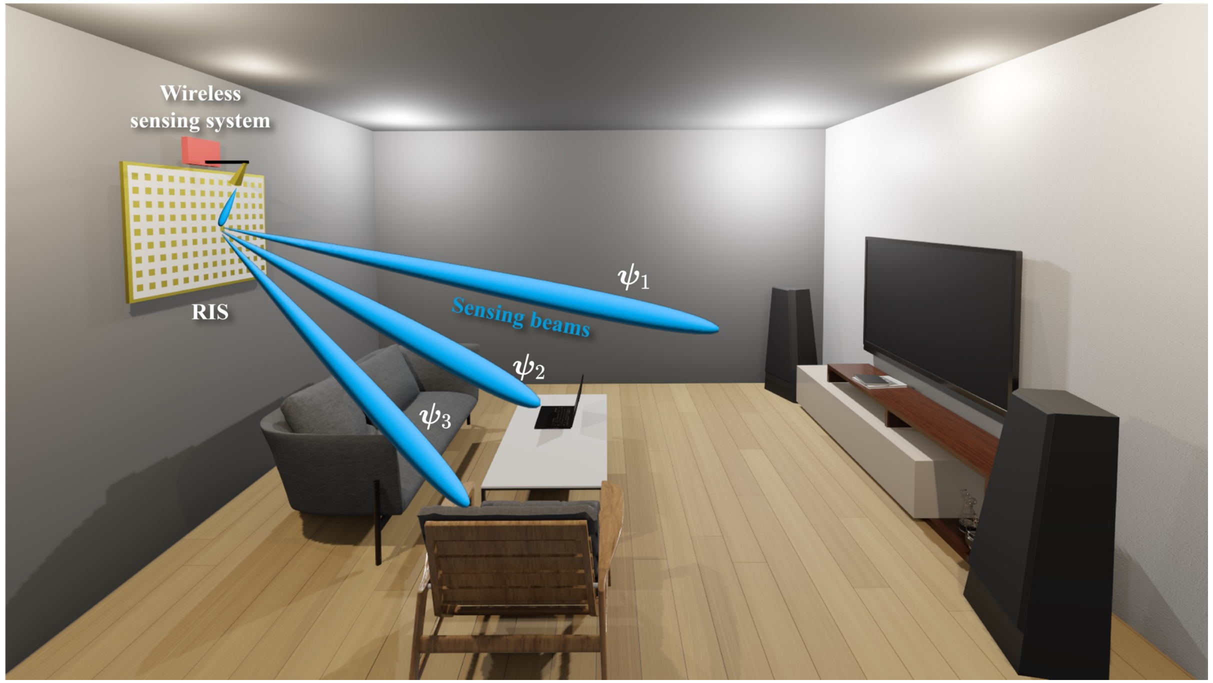

Proposed RIS-aided wireless sensing process for scene depth estimation

a) Sensing signals are transmitted to the RIS through a feeding antenna
b) RIS reflects incident signals to the environment
c) Backscattered/reflected signals are reflected by the RIS back to the sensing system
d) Receive signals are processed for scene depth estimation

Transmit signal model

Transmit signal (one chirp)

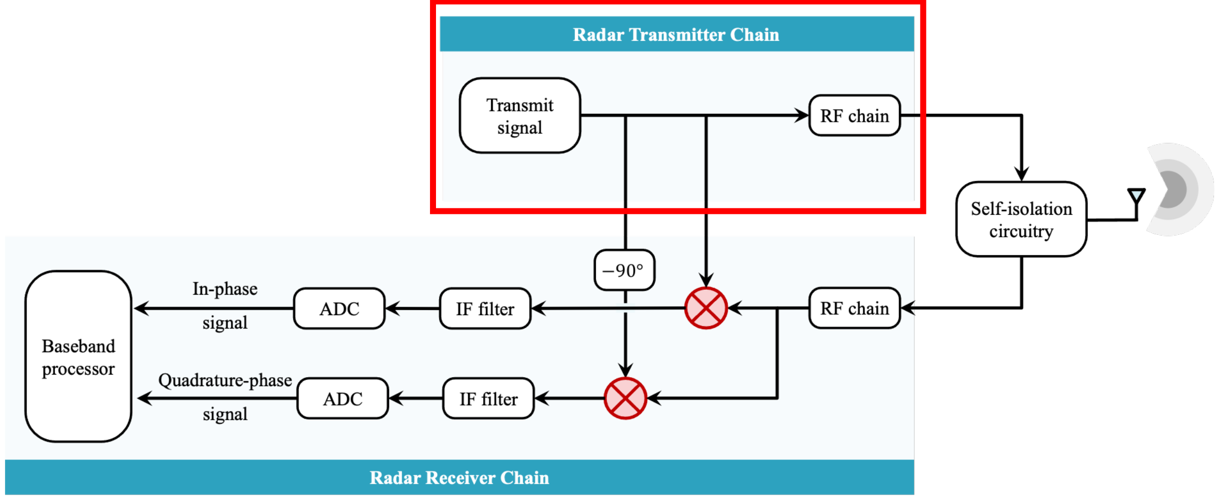

$$a_{\mathrm{BP}}(t) = \begin{cases} \cos\left(2\pi f_0 t + \pi S t^2\right) & 0 \le t \le T_{\text{active}}, \\ 0 & \text{otherwise.} \end{cases}$$

Starting frequency | Chirp slope | Active chirp time interval

$$\mathrm{BW} = \mathrm{S}T_{\text{active}}$$

Transmission bandwidth

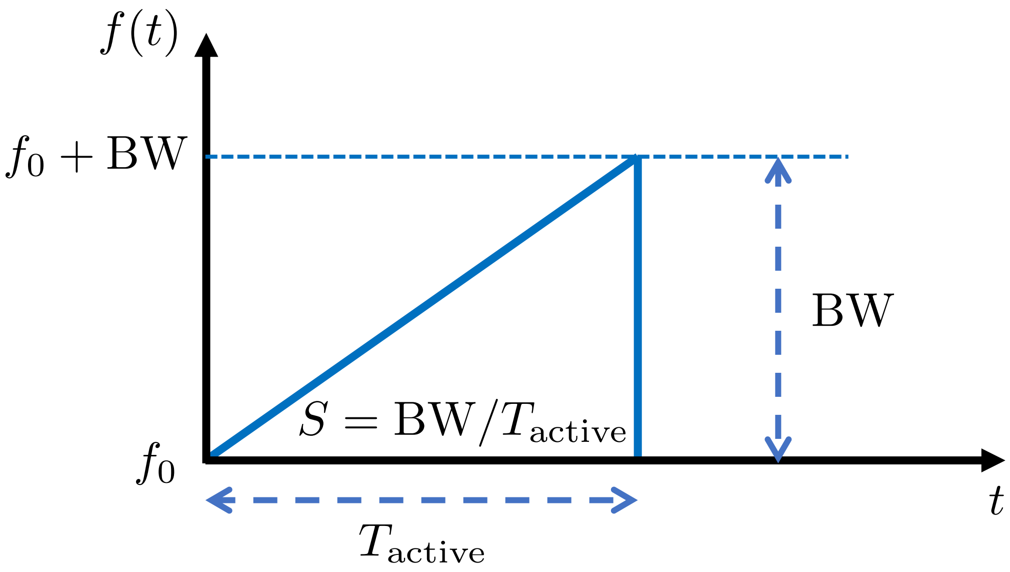

Transmit signal model

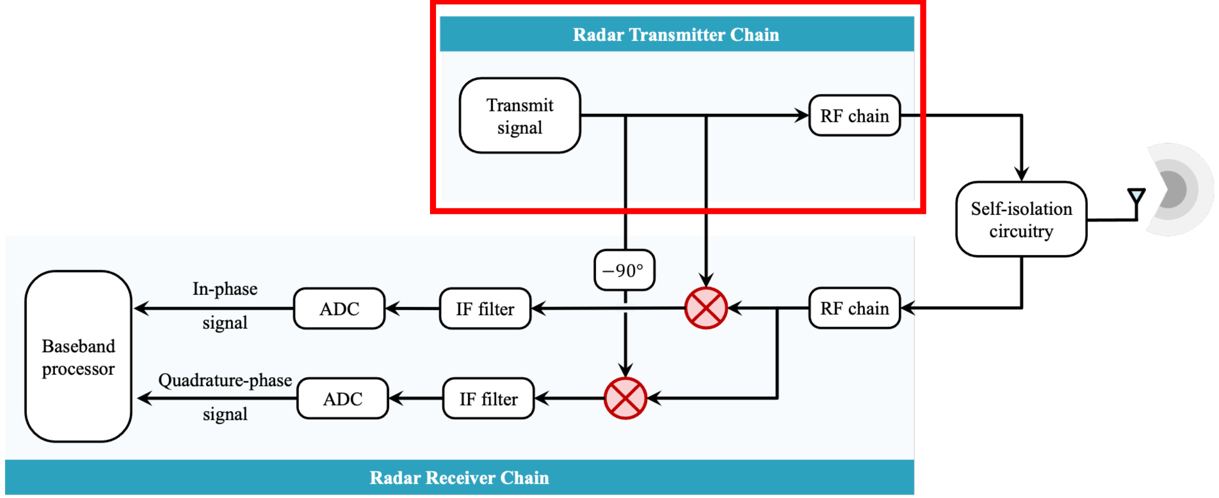

Transmit signal (one chirp)

$$a_{\mathrm{BP}}(t) = \begin{cases} \cos\left(2\pi f_0 t + \pi S t^2\right) & 0 \le t \le T_{\mathrm{active}}, \\ 0 & \text{otherwise.} \end{cases}$$

Starting frequency | Chirp slope | Active chirp time interval

$$\mathrm{BW} = \mathrm{S}T_{\mathrm{active}}$$

Transmission bandwidth

Transmit signal (one radar frame)

$$x_{\mathrm{BP}}(t) = \sqrt{\mathcal{E}_{\mathrm{T}}} \sum_{c=0}^{M_{\mathrm{chirp}}-1} a_{\mathrm{BP}}(t - cT_{\mathrm{PRI}})$$

$$= \mathrm{Re}\left(x(t)\, \mathrm{e}^{\jmath 2\pi f_0 t}\right), t \in \mathbb{R}_{\ge 0}$$

No. of chirps per frame

Chirp repetition interval

Transmission power

Complex-valued lowpass-equivalent transmit signal

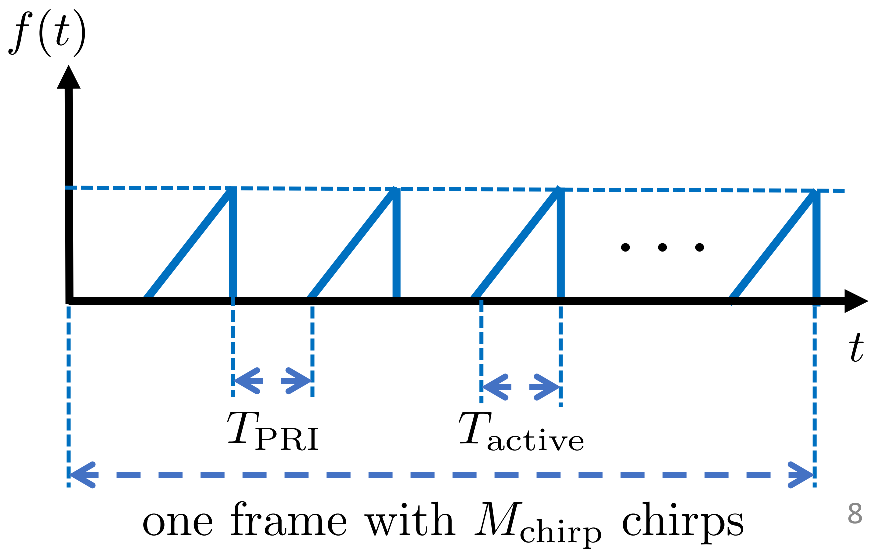

Receive signal model

Receive signal (one radar frame)

$$y_{\mathrm{BP}}(t) = \mathrm{Re}(y(t)\mathrm{e}^{\jmath 2\pi f_0 t})$$

Real-valued bandpass receive signal

Complex-valued lowpass-equivalent receive signal

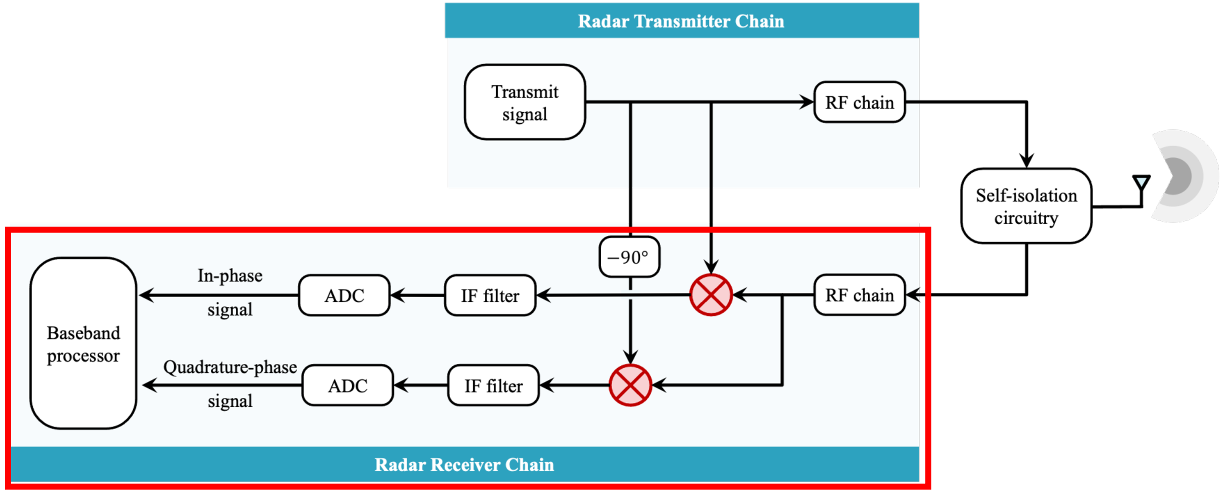

Receive signal model

Receive signal (one radar frame)

$$y_{\mathrm{BP}}(t) = \mathrm{Re}(y(t)\mathrm{e}^{\jmath 2\pi f_0 t})$$

No. targets

No. paths per target

$$y(t) = x(t) * h(t) + w(t) = \sum_{g=1}^{G_{\mathrm{tar}}} \sum_{\ell=1}^{L_g} \mathsf{h}_{g,\ell}(t) x(t - \xi_{g,\ell}) + w(t)$$

Lowpass-equivalent channel

Additive noise

Complex-valued channel path gain

$$\xi_{g,\ell} = R_{g,\ell}/\varsigma$$

Propagation delay

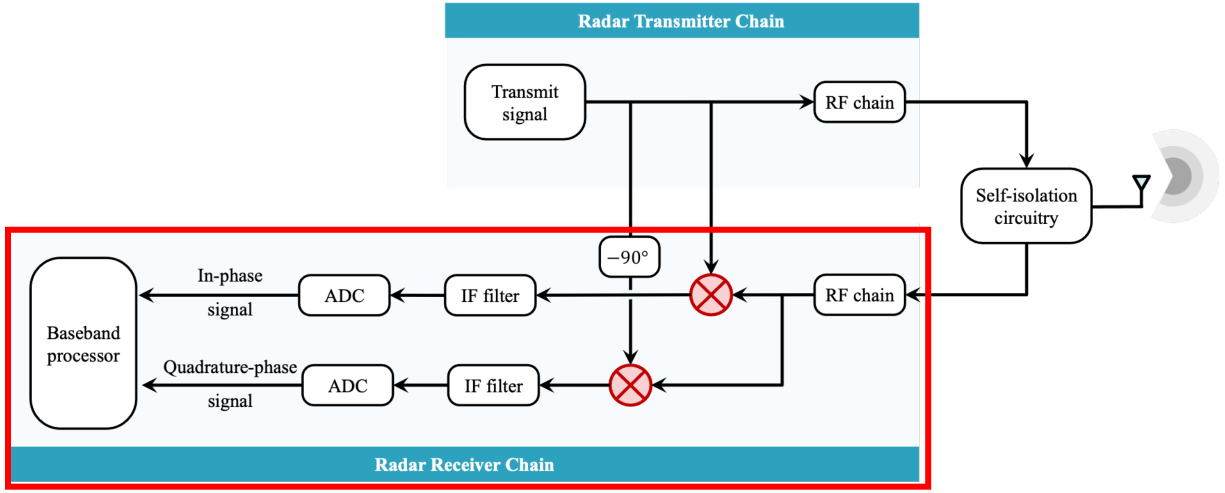

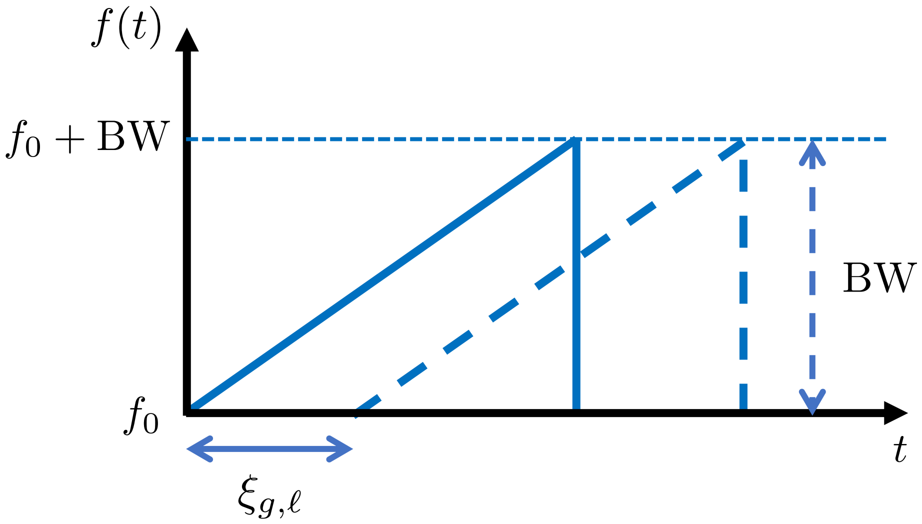

Receive signal model

Receive signal (one radar frame)

$$y_{\mathrm{BP}}(t) = \mathrm{Re}(y(t)e^{\jmath 2\pi f_0 t})$$

$$y(t) = x(t) * h(t) + w(t) = \sum_{g=1}^{G_{\mathrm{tar}}} \sum_{\ell=1}^{L_g} \mathsf{h}_{g,\ell}(t) x(t - \xi_{g,\ell}) + w(t)$$

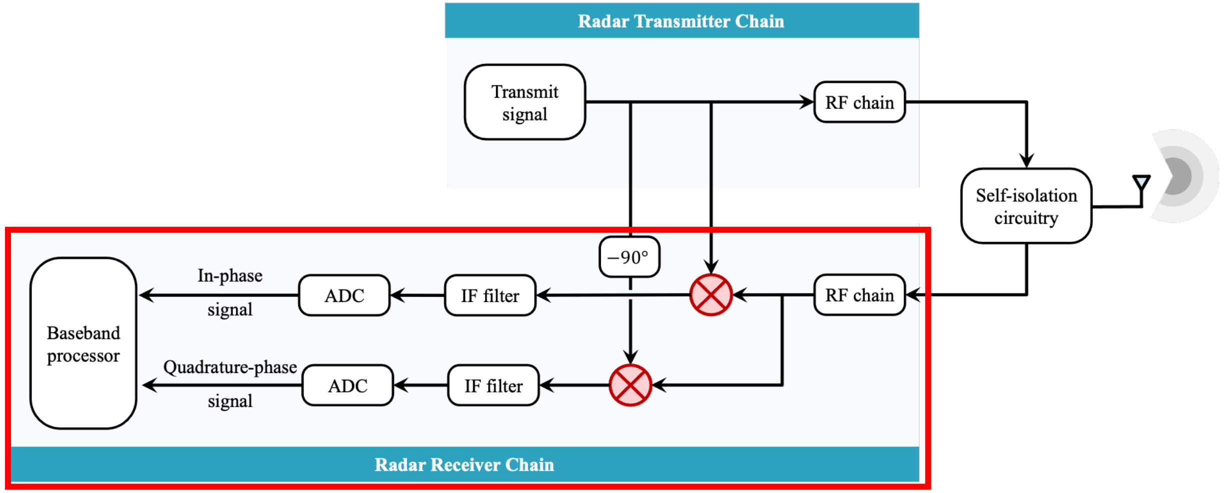

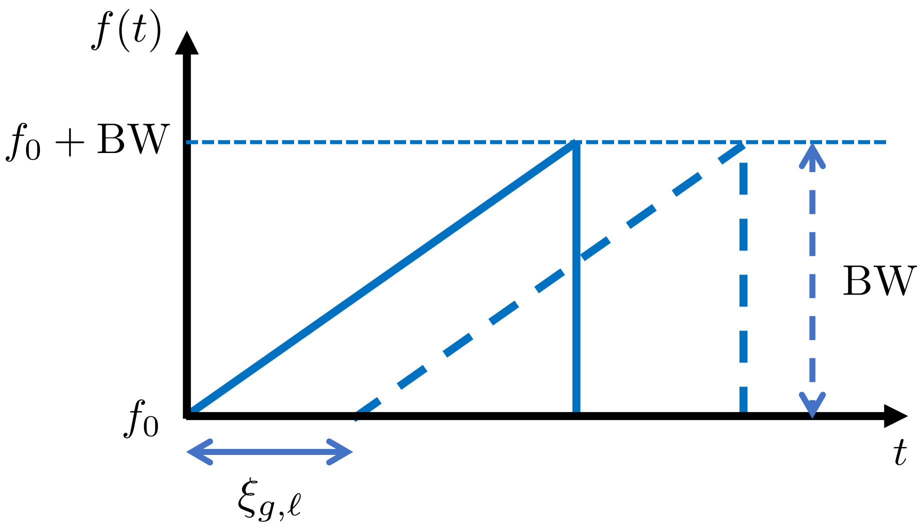

Receive baseband IF digital signal

After passing through the mixers, the filters and the ADCs

$$z[s, c] = I[s, c] + \jmath Q[s, c]$$

Sample index s
Chirp index c

In-phase signal

Quadrature signal

Receive signal model

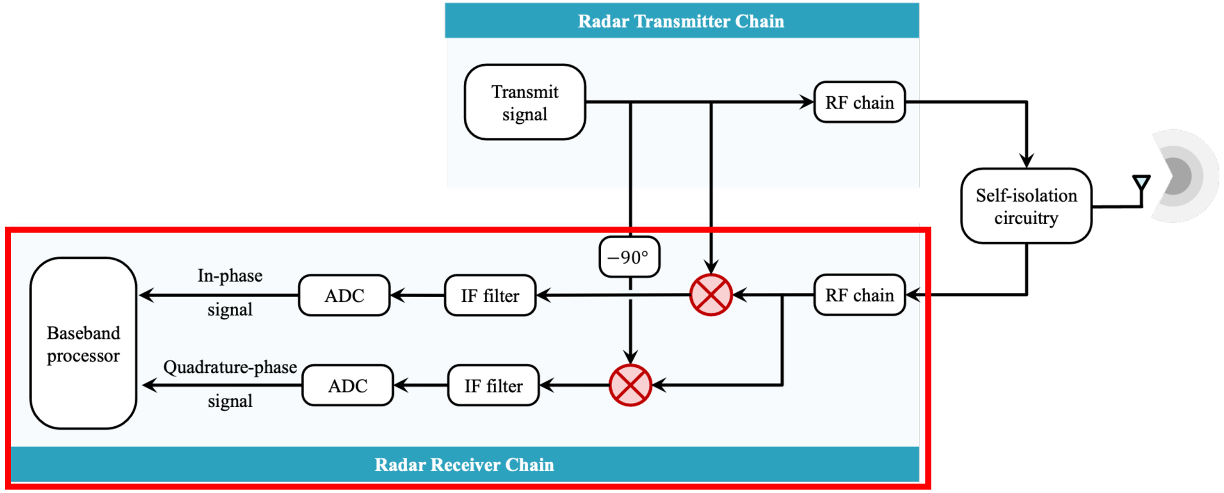

Receive signal (one radar frame)

$$y_{\mathrm{BP}}(t) = \mathrm{Re}(y(t)\mathrm{e}^{\jmath 2\pi f_0 t})$$

$$y(t) = x(t) * h(t) + w(t) = \sum_{g=1}^{G_{\mathrm{tar}}} \sum_{\ell=1}^{L_g} \mathsf{h}_{g,\ell}(t) x(t - \xi_{g,\ell}) + w(t)$$

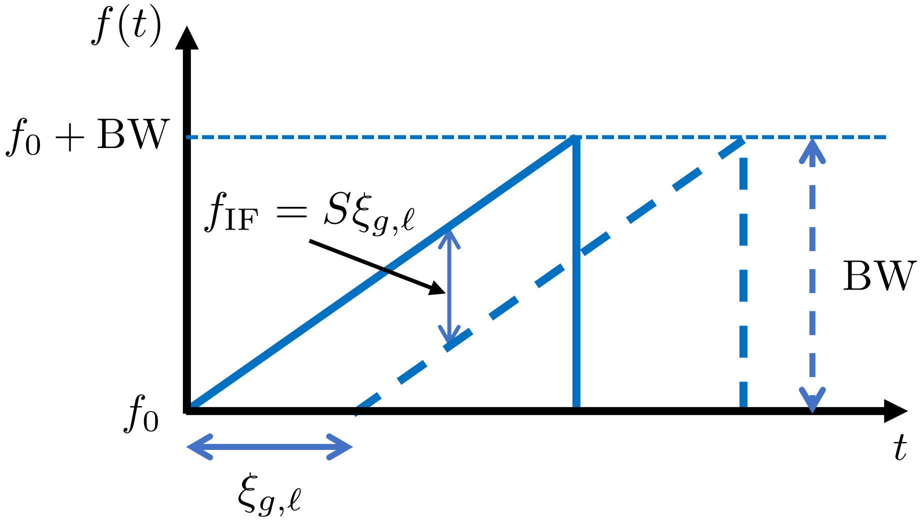

Receive baseband IF digital signal

After passing through the mixers, the filters and the ADCs

$$z[s,c] = I[s,c] + \jmath Q[s,c]$$

$$z[s,c] = \sum_{g=1}^{\mathsf{G}_{\mathrm{tar}}} \sum_{\ell=1}^{L} \sqrt{\rho_{g,\ell}}\, \mathrm{e}^{-\jmath \vartheta_{g,\ell}}\, \mathrm{e}^{+\jmath \Xi_{g,\ell}} + w[s,c]\mathrm{e}^{\jmath \chi[s]} \longleftarrow \chi[s] = 2\pi f_0 t_{\mathrm{fast}} + \pi S t_{\mathrm{fast}}^2$$

$$t_{\mathrm{fast}} = s T_{\mathrm{S}}$$

receive power of a single path

$$\rho_{g,\ell} = \mathcal{E}_{\mathrm{T}} |\mathsf{h}_{g,\ell}|^2$$

receive phase of a single path

$$\vartheta_{g,\ell} = \arg(\mathsf{h}_{g,\ell})$$

Phase term contains range information

$$\Xi_{g,\ell} = 2\pi \left(f_0 \xi_{g,\ell} + \underline{S t_{\mathrm{fast}} \xi_{g,\ell}} - \frac{S}{2} \xi_{g,\ell}^2 \right)$$

Propagation delay

$$\xi_{g,\ell} = R_{g,\ell} / \varsigma$$

Channel model

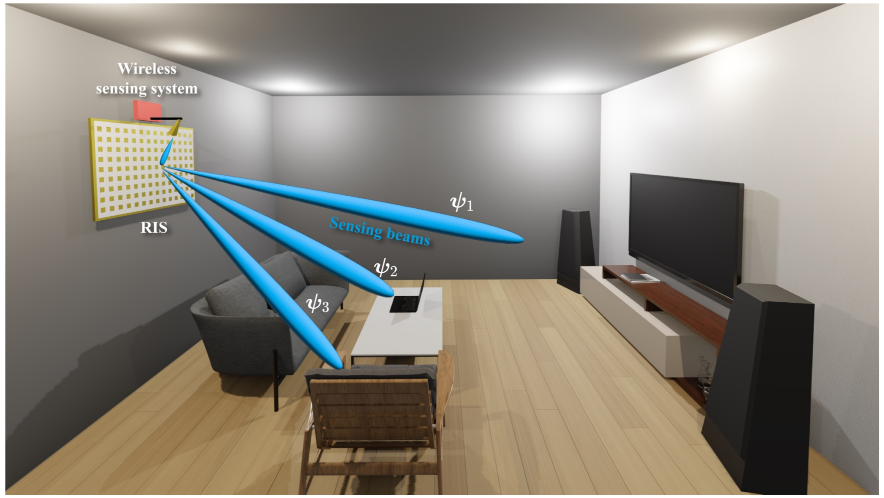

RIS interaction matrix

$$\mathsf{h}_{g,\ell}(t) = \underbrace{(\mathbf{g}^T \boldsymbol{\Psi} \mathbf{v}(\bar{\theta}_{g,\ell}(t))\bar{\gamma}_{g,\ell}(t))}_{\text{Radar}\to\text{RIS}\to\text{Target}} \times \underbrace{(\mathbf{g}^T \boldsymbol{\Psi} \mathbf{v}(\ddot{\theta}_{g,\ell}(t))\ddot{\gamma}_{g,\ell}(t))}_{\text{Target}\to\text{RIS}\to\text{Radar}}$$

Forward channel path gain

Backward channel path gain

Channel bet. RIS and radar antenna

Far-field array response vector bet. RIS and target

Assumptions

- RIS is equipped with N reconfigurable elements (phase shifters) → Not mutually correlated
- Channel between the RIS and the radar transceiver → Near-field channel
- Channel between the RIS and the targets → Far-field channel
- Channel between the radar transceiver and the targets → Neglected (directional rad. pattern of the feeding ant.)
- Reciprocal RIS interaction (incident signal directions ↔ reflected signal directions)

Problem definition: How to construct depth maps?

1. Scanning the environment using RIS interaction vectors

- Beam codebook $\mathcal{F}$: M RIS interaction vectors for M directions

$$\mathcal{F} = \{\boldsymbol{\psi}_m : m \in \mathcal{M}, \mathcal{M} = \{0, \ldots, M-1\}\}$$

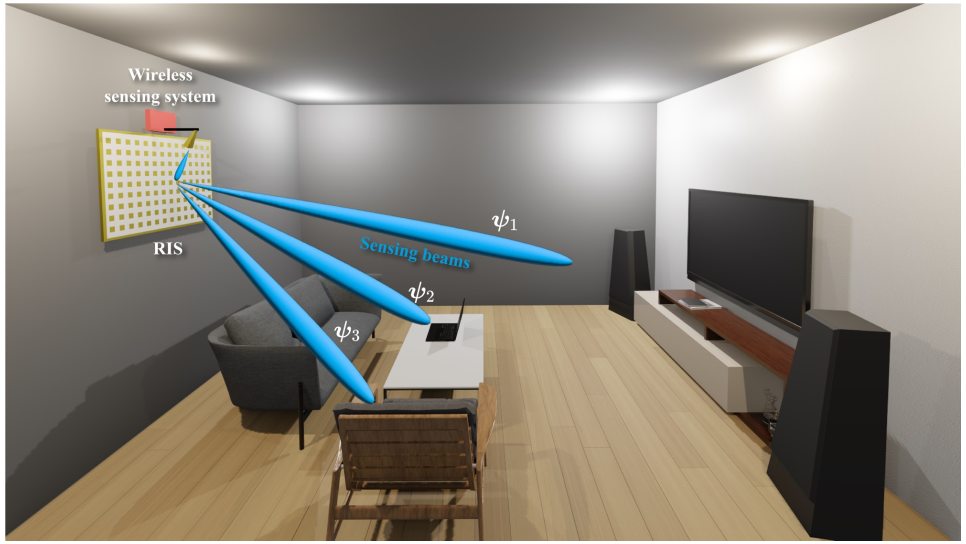

- For each interaction vector, the channel and IF signal models:

$$\mathsf{h}_{g,\ell}[m] = \bar{\gamma}_{g,\ell}\left((\mathbf{g} \odot \boldsymbol{\psi}_m)^T \mathbf{v}\left(\bar{\theta}_{g,\ell}\right)\right) \times \ddot{\gamma}_{g,\ell}\left((\mathbf{g} \odot \boldsymbol{\psi}_m)^T \mathbf{v}\left(\ddot{\theta}_{g,\ell}\right)\right)$$

$$z[s,m] = \underbrace{\sum_{g=1}^{\mathsf{G}_{\mathrm{tar}}} \sum_{\ell=1}^{L} \sqrt{\rho_{g,\ell}[m]}\, \mathbf{e}^{-\jmath \vartheta_{g,\ell}[m]}\, \mathbf{e}^{+\jmath\, \Xi_{g,\ell}}}_{\text{Receive signal}} + \underbrace{w[s,m]\mathbf{e}^{\jmath \chi[s]}}_{\text{Noise}}$$

- Received sensing signal matrix

$$\mathbf{z}[m] = [z[0,m], \ldots, z[M_{\mathrm{sample}} - 1, m]]^T$$

$$\mathbf{Z} = [\mathbf{z}[0], \mathbf{z}[1], \ldots, \mathbf{z}[M-1]]$$

Problem definition: How to construct depth maps?

2. Processing the receive signals to construct depth maps

- Ground-truth depth map, $\mathbf{D}_{\text{map}}$: 2D image of depth values

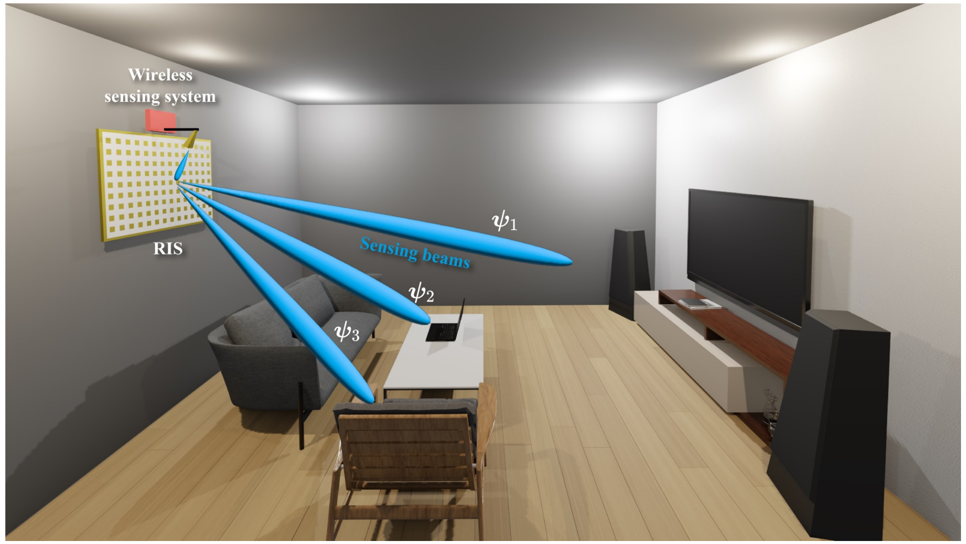

- Depth value in one direction:

  Smallest depth bet. RIS reference element and the nearest target

- Estimated depth map, $\widehat{\mathbf{D}}_{\text{map}}$: $\widehat{\mathbf{D}}_{\text{map}} = \mathbf{p}(\mathbf{Z}; \mathcal{F})$

- Estimation performance metrics
  - Root-mean squared error (RMSE) $\Delta_{\text{RMSE}} = \left(\frac{1}{M} \|\mathbf{D}_{\text{map}} - \mathbf{p}(\mathbf{Z}; \mathcal{F})\|_2^2 \right)^{1/2}$
  - Mean absolute error (MAE) $\Delta_{\text{MAE}} = \frac{1}{M} \|\mathbf{D}_{\text{map}} - \mathbf{p}(\mathbf{Z}; \mathcal{F})\|_1^2$

How can we design the sensing framework to reduce the est. errors?

Proposed solution: RIS interaction codebook design

- We adopt the design for the set of reflected angle directions, $\mathcal{O}$ [Taha'21]
  - Inputs: field of view, aspect ratio, horizontal and vertical resolutions
  - Output: the set of reflected angle directions for a rectangular grid

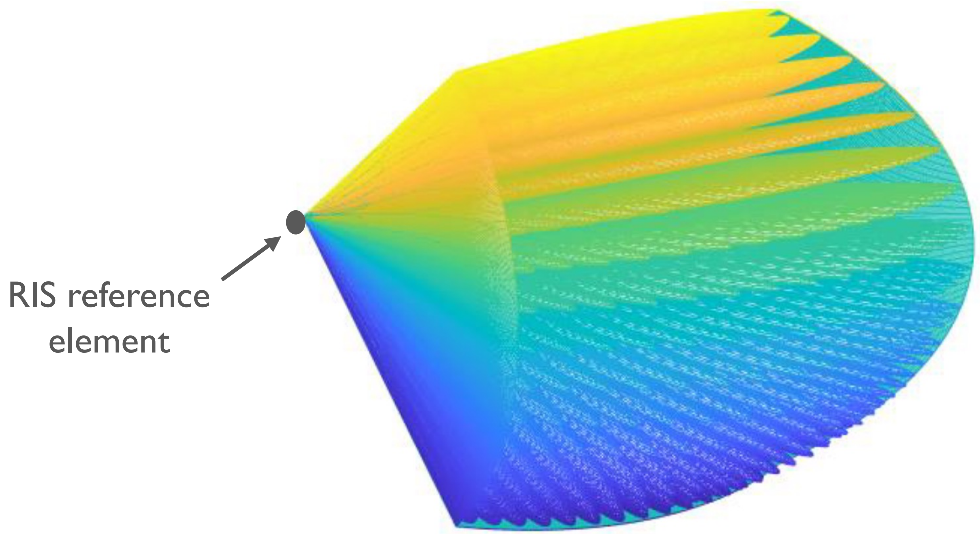

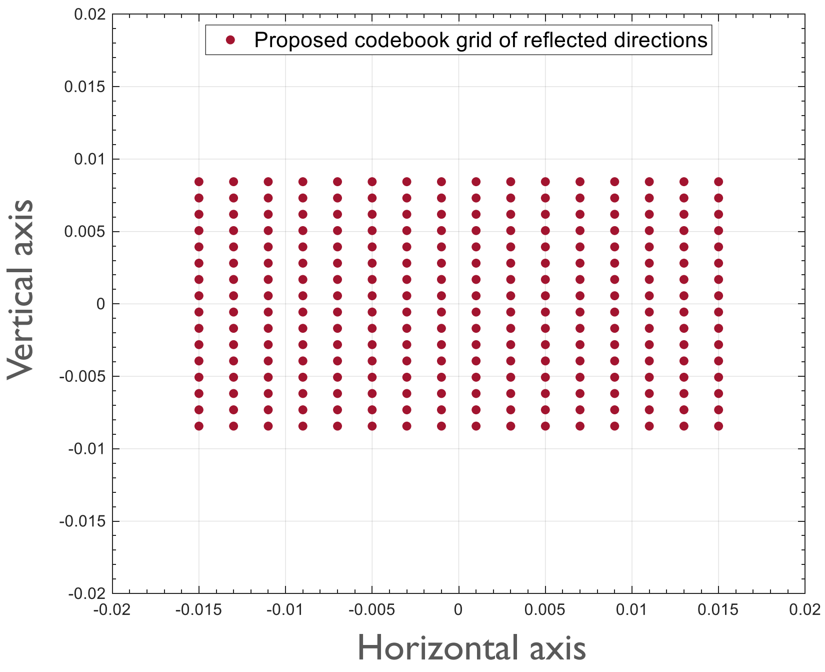

[Taha'21] A. Taha, Q. Qu, S. Alex, P. Wang, W. L. Abbott and A. Alkhateeb, "Millimeter Wave MIMO-Based Depth Maps for Wireless Virtual and Augmented Reality," in *IEEE Access*, vol. 9, pp. 48341-48363, 2021.

Proposed solution: RIS interaction codebook design

- We adopt the design for the set of reflected angle directions, $\mathcal{O}$ [Taha'21]
  - Inputs: field of view, aspect ratio, horizontal and vertical resolutions
  - Output: the set of reflected angle directions for a rectangular grid

- For $\theta_m \in \mathcal{O}$, the RIS interaction vector can be designed as

$$\boldsymbol{\psi}_m^\star = \arg\max_{\boldsymbol{\psi}_m} \; |\mathsf{h}_{g,\ell}[m]| \quad \text{s.t.} \; |[\boldsymbol{\psi}_m]_n| = 1, \; \forall n \in \{1, \ldots, N\}$$

$$\boldsymbol{\psi}_m^\star = \left(\mathbf{v}(\theta_m) \odot \mathrm{e}^{-\jmath 2\pi(\boldsymbol{\delta} - \delta_1)/\lambda}\right)^*, \; m \in \mathcal{M}$$

Prior knowledge
- The distance vector $\boldsymbol{\delta}$ bet. Radar antenna and RIS elements
- The direction specified by θ_m

- The proposed RIS interaction codebook

$$\mathcal{F} = \left\{\boldsymbol{\psi}_m \in \mathbb{C}^{N\times 1} : \boldsymbol{\psi}_m = (\mathbf{v}(\theta_m) \odot \mathrm{e}^{-\jmath 2\pi(\boldsymbol{\delta} - \delta_1)/\lambda})^*, \theta_m \in \mathcal{O}\right\}$$

Given the designed RIS codebook, we next present the scene depth estimation solution

[Taha'21] A. Taha, Q. Qu, S. Alex, P. Wang, W. L. Abbott and A. Alkhateeb, "Millimeter Wave MIMO-Based Depth Maps for Wireless Virtual and Augmented Reality," in *IEEE Access*, vol. 9, pp. 48341-48363, 2021.

Proposed solution: RIS-based scene depth estimation

Operation

- Acquire received sensing matrix
- Estimate range vector (Fourier transform)

$$\mathbf{Z}^{\mathrm{RP}} = \mathrm{FFT}_m\left(\mathbf{Z}\right), m \in \mathcal{M}$$

$$[\hat{\mathbf{r}}]_m = \Delta_{\mathrm{R}} \times \arg\max_s \left| \left[\mathbf{Z}^{\mathrm{RP}}\right]_{s,m} \right|, m \in \mathcal{M}$$

- Construct scene depth map [Taha'21]
- Apply 2D interpolation to scale the depth maps

Algorithm 1 RIS-Based Scene Depth Estimation Solution

Inputs: Field of view FoV, aspect ratio A_{R},
number of horizontal/vertical grid points $\overline{N}_{\mathrm{H}}, \overline{N}_{\mathrm{V}}$.

Output: Depth map estimate $\widehat{\mathbf{D}}_{\mathrm{map}}$.

1: Design RIS interaction codebook $\boldsymbol{\mathcal{F}}$, as in Section IV-B.
2: **for** $m = 1$ **to** M **do** ▷ For each $\boldsymbol{\psi}_m$
3: Acquire receive *sensing* signal $z[s, m]$, $\forall s \in \mathcal{S}$, (14).
4: Construct receive *sensing* matrix $\mathbf{Z}$, as in (15).
5: Calculate scene range estimate vector $\hat{\mathbf{r}}$, as in (32).
6: Construct the range map estimate $\widehat{\mathbf{R}}_{\mathrm{map}}$, as in (33).
7: Construct the depth map estimate $\widehat{\mathbf{D}}_{\mathrm{map}}$, as in [6].

[Taha'21] A. Taha, Q. Qu, S. Alex, P. Wang, W. L. Abbott and A. Alkhateeb, "Millimeter Wave MIMO-Based Depth Maps for Wireless Virtual and Augmented Reality," in *IEEE Access*, vol. 9, pp. 48341-48363, 2021.

Simulation framework

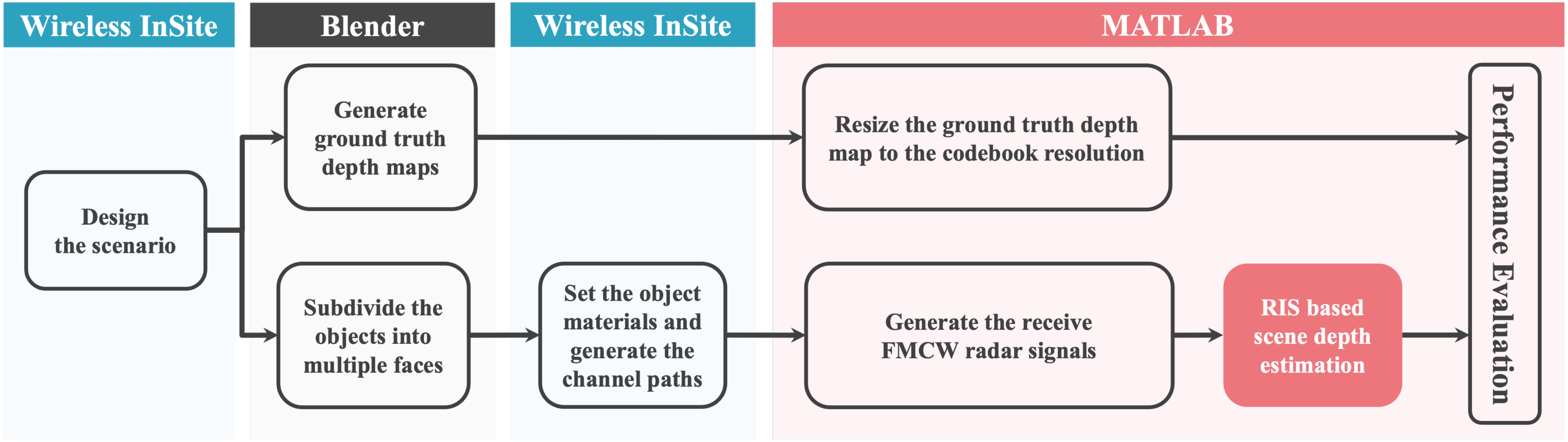

- Wireless InSite: $0.1°$ ray spacing. Enabled interactions: reflection, diffraction, transmission, diffuse scattering
- $\{30\times30;\ 40\times40\}$ RIS uniform planar arrays (UPAs) at 60GHz with 4GHz transmission bandwidth
- Codebook: oversampling factors of 4, size of $\{14{,}400; 25{,}600\}$
- $100°$ field of view, $4/3$ aspect ratio, 480p resolution, 32mm sensor width (ground-truth depth map)
- Assuming 38Msps sampling rate, 512 samples per chirp, and $13.47\mu s$ chirp repetition interval
- Estimate depth map sensing rate $\{5.15; 2.90\}$ Hz

Living room scenario

- 15.6×6.5×3.8m indoor space
  - 1.8m tall person
  - Concrete for the walls
  - Floorboard for the floor
  - Ceiling board for the ceiling
  - Glass material for the wall dividing the space
  - Glass material for the TV
  - Wood for the furniture
- Follow ITU default parameter values for the materials at 60GHz
- The RIS is mounted on the wall behind the sofa

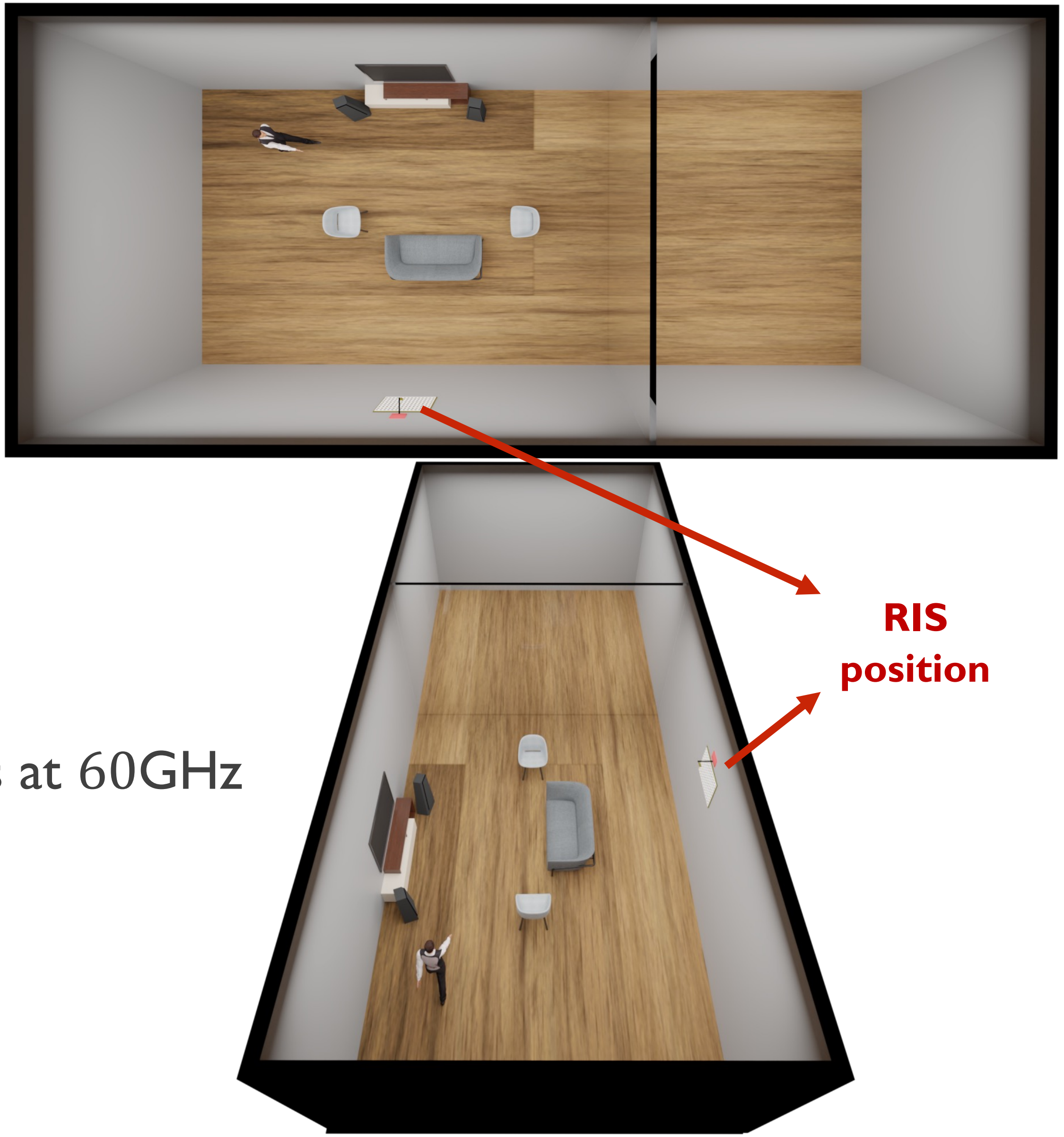

We compare the proposed solution against RGB-based solutions for depth estimation

Living room scenario (cont.)

RGB-based solutions

- Construct the shape of the objects more clearly
- Mis-detect the transparent glass wall
- Higher depth errors compared to ground truth

Proposed RIS-based solutions

- Transparent glass wall can be well perceived
- Lower depth errors compared to ground truth
- Suffer from some inter-path interferences
- Relatively wide sensing beams (errors around the edges)

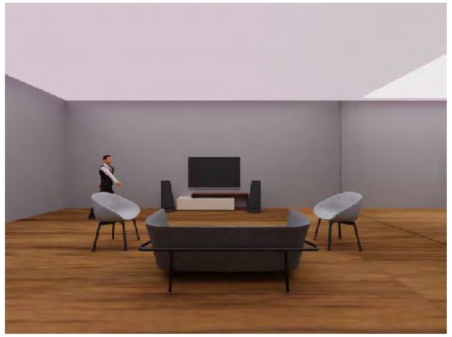

(a) RGB scene image

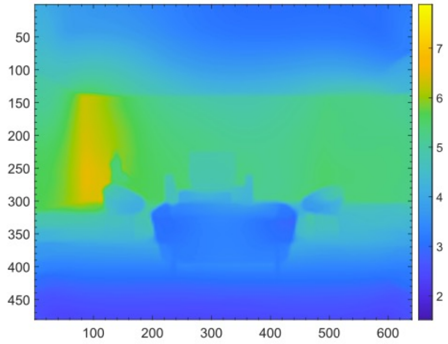

(b) RGB-based depth map [Hu'19]
$\Delta_{\mathrm{RMSE}} = 94.5\,\mathrm{cm}$
$\Delta_{\mathrm{MAE}} = 82.9\,\mathrm{cm}$

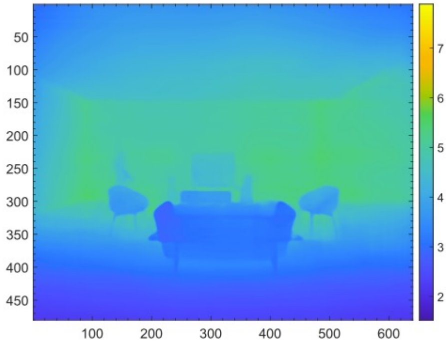

(c) RGB-based depth map [Ranftl'21]
$\Delta_{\mathrm{RMSE}} = 98.3\,\mathrm{cm}$
$\Delta_{\mathrm{MAE}} = 86.6\,\mathrm{cm}$

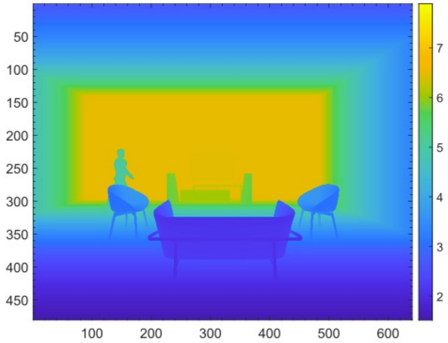

(d) Ground truth depth map

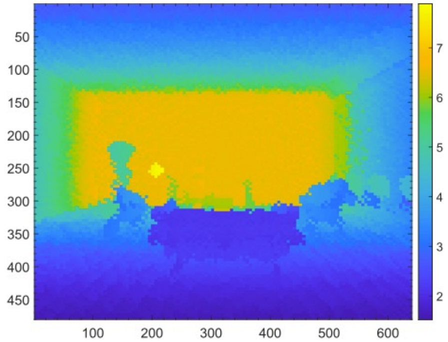

(e) Proposed sol. (30×30 RIS)
$\Delta_{\mathrm{RMSE}} = 37.5\,\mathrm{cm}$
$\Delta_{\mathrm{MAE}} = 14.5\,\mathrm{cm}$

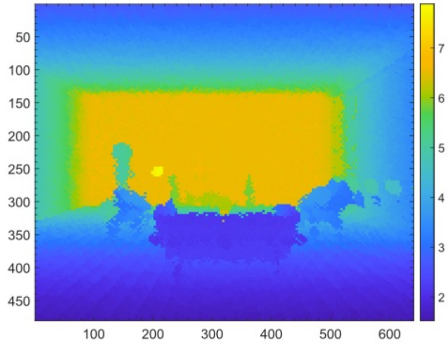

(f) Proposed sol. (40×40 RIS)
$\Delta_{\mathrm{RMSE}} = 31.9\,\mathrm{cm}$
$\Delta_{\mathrm{MAE}} = 11.6\,\mathrm{cm}$

The proposed solution can achieve higher depth accuracy

[Hu'19] Junjie Hu, Mete Ozay, Yan Zhang, and Takayuki Okatani. "Revisiting single image depth estimation: Toward higher resolution maps with accurate object boundaries." In 2019 IEEE Winter Conference on Applications of Computer Vision (WACV), pp. 1043-1051. IEEE, 2019.
[Ranftl'21] René Ranftl, Alexey Bochkovskiy, and Vladlen Koltun. "Vision transformers for dense prediction." In Proceedings of the IEEE/CVF International Conference on Computer Vision, pp. 12179-12188. 2021.

Conclusions and future work

- Optical sensing for depth perception suffers from critical limitations
  - Shiny, dark, transparent, or distant objects/surfaces
  - Key privacy concerns
  - Around-the-corner objects/surfaces
- RIS-aided mmWave sensing framework for scene depth estimation
  - Design a depth map suitable RIS sensing codebook
  - Develop a processing solution to estimate high-resolution depth maps
  - Simulation results highlight the potential of this solution to achieve accurate depth perception
- Future work
  - Improve the *precision* of the proposed solutions
  - Extend to near-field channels between RIS and targets
  - Adopt target mobility, i.e., depth and Doppler velocity estimation

Thank you

Appendix

Channel model

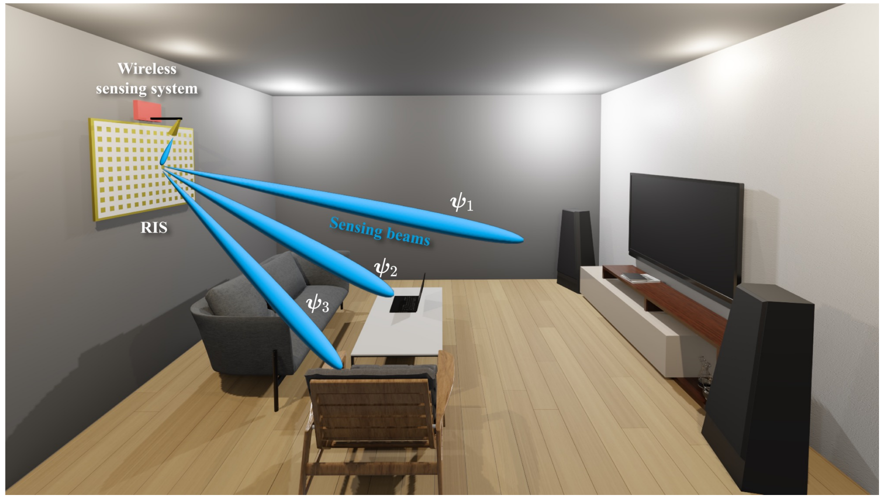

Backward from the target

$$\mathsf{h}_{g,\ell}(t) = \underbrace{(\mathbf{g}^T \boldsymbol{\Psi} \mathbf{v}(\bar{\theta}_{g,\ell}(t))\bar{\gamma}_{g,\ell})(t)}_{\text{Radar}\rightarrow\text{RIS}\rightarrow\text{Target}} \times \underbrace{(\mathbf{g}^T \boldsymbol{\Psi} \mathbf{v}(\ddot{\theta}_{g,\ell}(t))\ddot{\gamma}_{g,\ell}(t))}_{\text{Target}\rightarrow\text{RIS}\rightarrow\text{Radar}}$$

Forward to the target

[Buzzi'21] S. Buzzi, E. Grossi, M. Lops, and L. Venturino, "Foundations of MIMO Radar Detection Aided by Reconfigurable Intelligent Surfaces," *IEEE Transactions on Signal Processing*, vol. 70, pp. 1749–1763, 2022.

Channel model

RIS interaction matrix

$$\mathsf{h}_{g,\ell}(t) = \underbrace{(\mathbf{g}^T \mathbf{\Psi} \mathbf{v}(\bar{\theta}_{g,\ell}(t))\bar{\gamma}_{g,\ell})(t)}_{\text{Radar}\to\text{RIS}\to\text{Target}} \times \underbrace{(\mathbf{g}^T \mathbf{\Psi} \mathbf{v}(\ddot{\theta}_{g,\ell}(t))\ddot{\gamma}_{g,\ell}(t))}_{\text{Target}\to\text{RIS}\to\text{Radar}}$$

Forward channel path gain

Backward channel path gain

Channel bet. RIS and radar antenna

Far-field array response vector bet. RIS and target

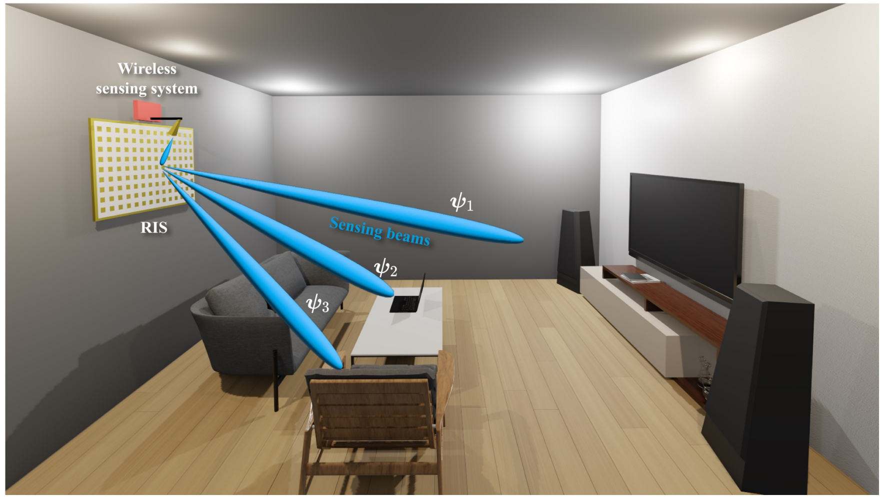

[Buzzi'21] S. Buzzi, E. Grossi, M. Lops, and L. Venturino, "Foundations of MIMO Radar Detection Aided by Reconfigurable Intelligent Surfaces," *IEEE Transactions on Signal Processing*, vol. 70, pp. 1749–1763, 2022.

Channel model

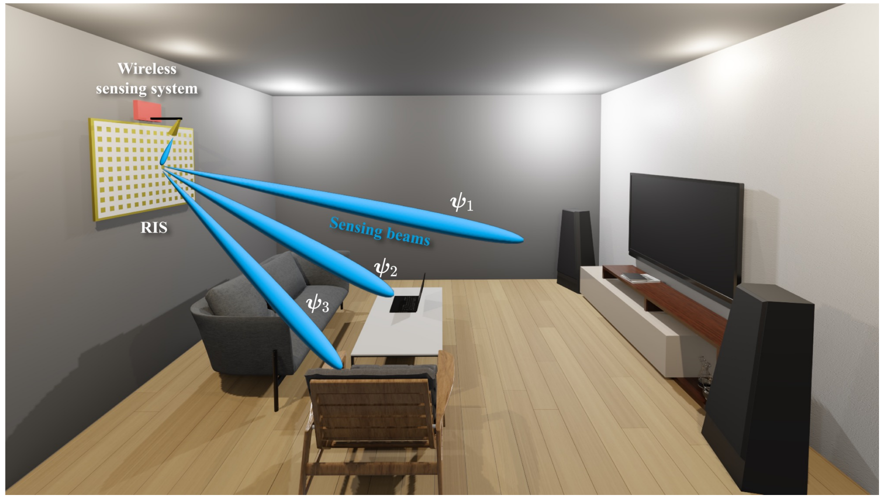

$$\mathsf{h}_{g,\ell}(t) = \underbrace{(\mathbf{g}^T \boldsymbol{\Psi} \mathbf{v}(\bar{\theta}_{g,\ell}(t))\bar{\gamma}_{g,\ell})(t)}_{\text{Radar}\to\text{RIS}\to\text{Target}} \times \underbrace{(\mathbf{g}^T \boldsymbol{\Psi} \mathbf{v}(\ddot{\theta}_{g,\ell}(t))\ddot{\gamma}_{g,\ell}(t))}_{\text{Target}\to\text{RIS}\to\text{Radar}}$$

$$= \bar{\gamma}_{g,\ell}(t) \left((\mathbf{g} \odot \boldsymbol{\psi})^T \mathbf{v}\left(\bar{\theta}_{g,\ell}(t)\right) \right) \times \ddot{\gamma}_{g,\ell}(t) \left((\mathbf{g} \odot \boldsymbol{\psi})^T \mathbf{v}\left(\ddot{\theta}_{g,\ell}(t)\right) \right)$$

RIS interaction vector

[Buzzi'21] S. Buzzi, E. Grossi, M. Lops, and L. Venturino, "Foundations of MIMO Radar Detection Aided by Reconfigurable Intelligent Surfaces," *IEEE Transactions on Signal Processing*, vol. 70, pp. 1749–1763, 2022.

Channel model

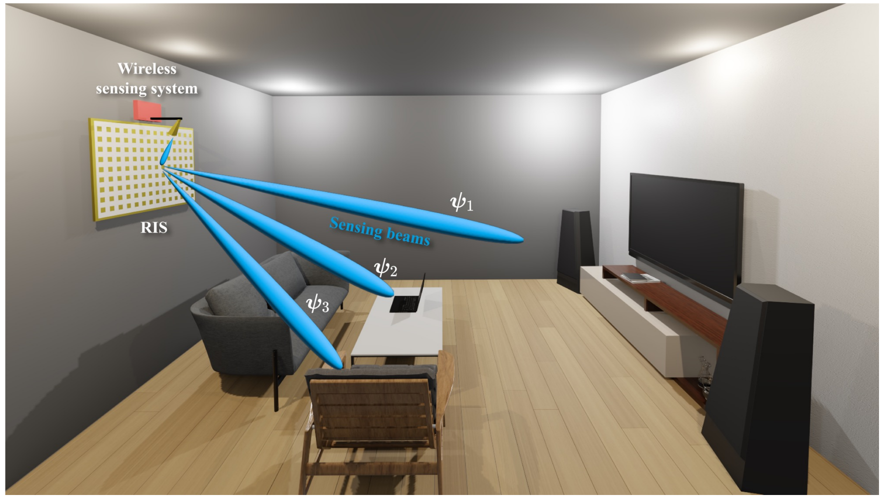

$$\mathsf{h}_{g,\ell}(t) = \underbrace{(\mathbf{g}^T \boldsymbol{\Psi} \mathbf{v}(\bar{\theta}_{g,\ell}(t))\bar{\gamma}_{g,\ell})(t)}_{\text{Radar}\rightarrow\text{RIS}\rightarrow\text{Target}} \times \underbrace{(\mathbf{g}^T \boldsymbol{\Psi} \mathbf{v}(\ddot{\theta}_{g,\ell}(t))\ddot{\gamma}_{g,\ell}(t))}_{\text{Target}\rightarrow\text{RIS}\rightarrow\text{Radar}}$$

$$= \bar{\gamma}_{g,\ell}(t)\left((\mathbf{g}\odot\boldsymbol{\psi})^T \mathbf{v}\left(\bar{\theta}_{g,\ell}(t)\right)\right) \times \ddot{\gamma}_{g,\ell}(t)\left((\mathbf{g}\odot\boldsymbol{\psi})^T \mathbf{v}\left(\ddot{\theta}_{g,\ell}(t)\right)\right)$$

Two-hop forward and backward channel path gains

$$\bar{\gamma}_{g,\ell}(t) = \sqrt{\frac{\mathcal{G}(\bar{\Omega}_1)\zeta(\bar{\omega}_1,\bar{\theta}_{g,\ell})}{(4\pi)^2\delta_1^2\bar{d}_{g,\ell}^2(t)\bar{\mathsf{L}}_{g,\ell}(t)}}\ \mathrm{e}^{-\jmath 2\pi(\delta_1+\bar{d}_{g,\ell})/\lambda}$$

$$\ddot{\gamma}_{g,\ell}(t) = \sqrt{\frac{\sigma_g\zeta(\ddot{\theta}_{g,\ell},\ddot{\omega}_1)\mathcal{G}(\ddot{\Omega}_1)\lambda^2}{(4\pi)^3\ddot{d}_{g,\ell}^2(t)\delta_1^2\ddot{\mathsf{L}}_{g,\ell}(t)}}\ \mathrm{e}^{-\jmath 2\pi(\ddot{d}_{g,\ell}+\delta_1)/\lambda}$$

Radar range equation

- **Directional gain of feeding antenna**
- **Directional RIS cross-section gain**
- **Target cross-section gain**

- **Distance bet. RIS reference and target**
- **Distance bet. RIS reference and radar antenna**

[Bu ... ounc ... Surfaces," *IEEE Transactions on Sign* ...

Channel model

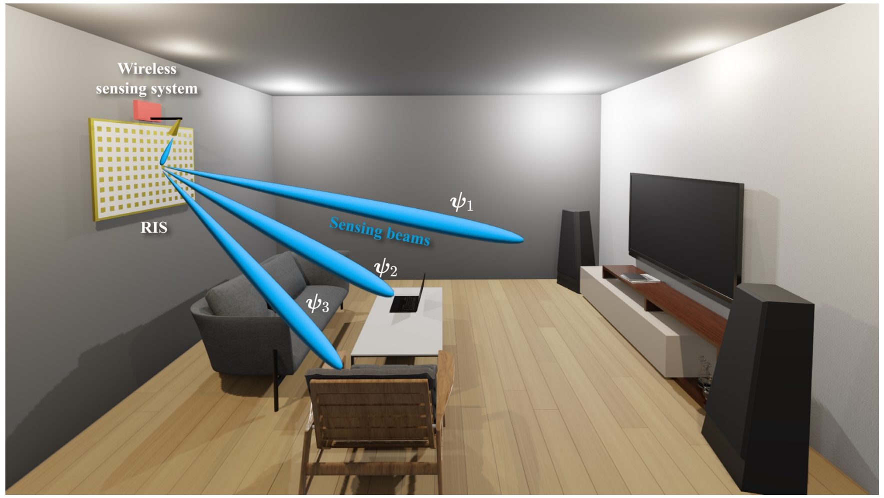

$$\mathsf{h}_{g,\ell}(t) = \underbrace{\left(\mathbf{g}^T \boldsymbol{\Psi} \mathbf{v}(\bar{\theta}_{g,\ell}(t))\bar{\gamma}_{g,\ell}\right)(t)}_{\text{Radar}\rightarrow\text{RIS}\rightarrow\text{Target}} \times \underbrace{\left(\mathbf{g}^T \boldsymbol{\Psi} \mathbf{v}(\ddot{\theta}_{g,\ell}(t))\ddot{\gamma}_{g,\ell}(t)\right)}_{\text{Target}\rightarrow\text{RIS}\rightarrow\text{Radar}}$$

$$= \bar{\gamma}_{g,\ell}(t)\left((\mathbf{g}\odot\boldsymbol{\psi})^T \mathbf{v}\left(\bar{\theta}_{g,\ell}(t)\right)\right) \times \ddot{\gamma}_{g,\ell}(t)\left((\mathbf{g}\odot\boldsymbol{\psi})^T \mathbf{v}\left(\ddot{\theta}_{g,\ell}(t)\right)\right)$$

Two-hop forward and backward channel path gains

$$\bar{\gamma}_{g,\ell}(t) = \sqrt{\frac{\mathcal{G}(\bar{\Omega}_1)\zeta(\bar{\omega}_1,\bar{\theta}_{g,\ell})}{(4\pi)^2\delta_1^2\bar{d}_{g,\ell}^2(t)\bar{\mathsf{L}}_{g,\ell}(t)}}\ \mathrm{e}^{-\jmath 2\pi(\delta_1+\bar{d}_{g,\ell})/\lambda}$$

$$\ddot{\gamma}_{g,\ell}(t) = \sqrt{\frac{\sigma_g\zeta(\ddot{\theta}_{g,\ell},\ddot{\omega}_1)\mathcal{G}(\ddot{\Omega}_1)\lambda^2}{(4\pi)^3\ddot{d}_{g,\ell}^2(t)\delta_1^2\ddot{\mathsf{L}}_{g,\ell}(t)}}\ \mathrm{e}^{-\jmath 2\pi(\ddot{d}_{g,\ell}+\delta_1)/\lambda}$$

Normalized near-field channel path gains

$$[\mathbf{g}]_n = \sqrt{\frac{\mathcal{G}(\bar{\Omega}_n)\zeta(\bar{\omega}_n,\bar{\theta}_{g,\ell})\delta_1^2}{\mathcal{G}(\bar{\Omega}_1)\zeta(\bar{\omega}_1,\bar{\theta}_{g,\ell})\delta_n^2}} \cdot \mathbf{e}^{-\jmath 2\pi(\delta_n-\delta_1)/\lambda}$$

$$\varphi = \{\varphi^{\mathrm{az}}, \varphi^{\mathrm{ze}}\}$$

Angle notation

Normalized gain for each RIS element w.r.t. RIS reference element

[Buzzi'21] S. Buzzi, E. Grossi, M. Lops, and L. Venturino, "Foundati … e Intelligent Surfaces," *IEEE Transactions on Signal Processing*, vol. 70, pp. 1749–1763, 2022.

FMCW radar configuration

- System configuration
  - 60 GHz starting frequency
  - Chirp slope: $300\ \mathrm{MHz}\ \mu\mathrm{s}^{-1}$
  - ADC sampling frequency: $38\ \mathrm{MS/s}$
  - 512 samples per chirp
  - $13.47\ \mu\mathrm{s}$ chirp repetition interval

- Derived parameters
  - $13.47\ \mu\mathrm{s}$ chirp duration
  - $4.04\ \mathrm{GHz}$ transmission bandwidth
  - Range resolution: $3.71\ \mathrm{cm}$
  - Maximum range: $18.95\ \mathrm{m}$
  - Chirp rate: $74.2\ \mathrm{kHz}$
  - RIS codebook size: $\{14{,}400; 25{,}600\}$
  - Depth map sensing rate: $\{5.15; 2.90\}\ \mathrm{Hz}$